



ORIGINAL ARTICLE

Numerical Modeling of Flow into Primary Dedusting System of a 130t Converter

Bruno Orlando de Almeida Santos¹, Breno Totti Maia^{1,*},
Fabrício Silveira Garajau¹, Marcelo de Souza Lima Guerra¹,
Hugo Leonardo de Freitas², José Geraldo Torres²,
Rudolf Huebner³, Roberto Parreiras Tavares³

¹Lumar Metals Research, Rod. MG 232 - Km 09, n.70, Santana do Paraíso, Brazil.

²Arcelor Mittal João Monlevade, Av. Getúlio Vargas, 100, Centro Industrial, João Monlevade, Minas Gerais, Brazil.

³Universidade Federal de Minas Gerais (UFMG), Av. Antônio Carlos, 6627, Pampulha, Belo Horizonte, Minas Gerais, Brazil.

Manuscript received February 6th, 2012; in revised form April 18, 2012

In this work an analysis of gases' behavior into primary dedusting system of basic oxygen furnace (BOF) converter was developed. The methodology involves Computational Fluid Dynamics (CFD) to simulate velocity, temperature of gases in combustion for multi-phases systems including solid particles. The influence of the air in the flow, analysis of temperature and gas along the dedusting system and the influence in cooling pipes was investigated. Numerical data were validated with real values of the process. The next step was the implementation of changes in the geometry of the ducts in order to find a more stable situation for the equipment. The best result was obtained by increasing the diameter and smoothing the geometries in curves.

KEY WORDS: Dedusting system; CFD; Temperature; Duct geometry

© 2012 Brazilian Metallurgical, Materials and Mining Association. Published by Elsevier Editora Ltda.

Este é um artigo Open Access sob a licença de [CC BY-NC-ND](http://creativecommons.org/licenses/by-nc-nd/4.0/)

1. Introduction

The dedusting system is a device to control air pollution with the function of taking flow gases and fine solids. The other function is to separate solids from gases. There are two mainly types: dry systems and wet systems. In this study, the 130 t LD converter presents these two system types. The primary dedusting is the wet system and is used to take the gases direct from the converter's mouth. The

secondary dedusting is the dry system and collects fumes around the converter.

The primary dedusting is responsible for collecting fumes that come from the oxygen blown into the metallic bath; at the same time, the secondary system is responsible to collect fumes from the hot metal charge and scrap into the converter and fugitives gases and fumes during blow^[1].

In the wet systems the gases are partially cooled by the cooling ducts. The next stages, Quencher and Venturi system, are important to separate the solids particles from de gas flow. Quencher is used to remove fraction of large diameter of particles in fumes and Venturi is used to remove

*Corresponding author.

E-mail address: breno.totti@lumarmetals.com.br (B.T. Maia)

fraction of small diameter. Together, Quencher and Venturi has the aim to guarantee the environmental law.

The fumes blow up from converter with high temperatures around 1,700°C. The solid part has high content of FeO, CaO, C, and other slag elements. These fumes enter into ducts together with air. The amount of air depends of the kind of the skirt that determines the suppress combustion when the skirt is movable or complete combustion when the skirt is fixed.

The hood and cooling stack are made with bundles of pipes welded together. Water circulates into the pipes to absorb the radiation and convection heat from gases by the pipe's wall. The mainly function of the heat transfer by the pipes is reduce temperature, and by this way, reduce the volume of fumes.

During the passage of fumes in the dedusting system, the contacts with cooling pipes promote convection in the wall pipes. The efficiency is a function of the correct water flow, water control temperature in the system's inlet and outlet, pressure and back pressure in the circuit, and water control quality. For the other side, the correct dimension of ducts and pipes guarantees correct residence time of fumes with adequate contact fume pipe wall, maximizing heat transfer.

The cooling water is pumped into system by closed and pressurized circuit. The heat is removed from the gases and dissipated to the air through heat exchanger. The circuit has tanks pressurized with nitrogen to obtain constant pressure and increase boiling temperature of water and permit to extract more heat from the system.

The gases, before cleaning, need to reduce temperature until around 900°C by the hood and the cooling stack. The exhaustion capacity is determined by the fan capacity and the respective system pressure drop. It is very important some excess in the fan capacity to consider any operational deviation^[2]. Other important factor in this first stage of the wet dedusting system is the duct geometry criteria. The aim is a uniform flow of fumes during the cooling duct^[3,4].

Numerical calculations from computational methods are tools that allow analyses of parameters described with the possibility of identify device problems in the project stage or during operation. It is a strong tool to help maintenance personnel, where the reason for most problems are, and help develop the best solution^[5-7].

2. Model Formulation

2.1. Governing Equation for Gas

The gas phase is described by transport equations of the continuous phase, being the Navier-Stokes equations solved by conservative form. The equations solved to gas phase include mass conservation, momentum, and turbulent kinetic energy, rate of turbulent dissipation, enthalpy, and chemical species.

The mass conservation and momentum equations are:

$$\frac{\partial \rho}{\partial t} + \nabla \cdot (\rho \vec{U}) = S_m$$

$$\frac{\partial}{\partial t} (\rho \vec{v}) + \nabla \cdot (\rho \vec{U} \vec{U}) = -\nabla p + \nabla \cdot \left(\vec{\tau} \right) + \rho \vec{g} + \vec{F}$$

where ρ is the gas density, U is the velocity, and the term S_m is the mass added in the continuous phase by the second disperse phase. The p term is the static pressure, stress tensor and are gravitational forces of body and external forces, respectively.

The energy equation is derivate of the first law of thermodynamic where the energy variation rate of one particle of fluid is equal to the heat rate to one particle of fluid added the work realized. For the steady stationary, the energy equation is solved as follows:

$$\frac{\partial (\rho h_{tot})}{\partial t} - \frac{\partial p}{\partial t} + \nabla \cdot (\rho \vec{v} h_{tot}) - \nabla \cdot (k \nabla T) + \nabla \cdot (\vec{v} \cdot \vec{\tau}) + \vec{v} \cdot \vec{S}_M + S_E$$

where $\nabla \cdot (\vec{v} \cdot \vec{\tau})$ term represents work by viscous tensions and $\vec{v} \cdot \vec{S}_M$ is work by external momentum forces, being normally neglected. The h_{tot} term is total enthalpy related with the static enthalpy h (T, p) by the equation:

$$h_{tot} = h + \frac{1}{2} v^2$$

The mixer model and chemical species transport are based in conservations equations that describe convection and diffusion sources and reactions for each chemical species. To solve the conservation equations is foreseen a region for each chemical specie, Y_i , through solution of the convection/diffusion equation for each chemical specie, which shows basic form like the equation below:

$$\frac{\partial}{\partial t} (\rho Y_i) + \nabla \cdot (\rho \vec{v} Y_i) = -\nabla \cdot \vec{J}_i + R_i + S_i$$

where R_i is the production rate of one chemical specie i . The reaction is calculated like the sum of reaction Arrhenius source over the number of reactions that the specie runs, showed in the equation. The term J_i is the diffusive flow of species i , which appears form gradients concentration and temperature.

$$R_i = M_{w,i} \sum_{r=1}^{N_R} \hat{R}_{i,r}$$

Turbulence model $k-\varepsilon$ is based on the model of transport equations to kinetic energy of turbulence (k), defined as variations in the velocity fluctuations, and the rate turbulence dissipation (ε), defined as the rate in which occurs the dissipation in the velocity fluctuations.

This model introduces two new variables in the system of equations, being based in the turbulent viscous concept μ_t , assuming that the turbulent viscous is linked with kinetic turbulent energy and dissipation, as shown in the equation:

$$\mu_t = C_\mu \rho \frac{k^2}{\varepsilon}$$

The k and ε values are obtained from differential equations of transport, in equations of the form of:

$$\frac{\partial (\rho k)}{\partial t} + \frac{\partial}{\partial x_j} (\rho U_j k) = \frac{\partial}{\partial x_j} \left[\left(\mu + \frac{\mu_t}{\sigma_k} \right) \frac{\partial k}{\partial x_j} \right] + P_k - \rho \varepsilon + P_{kb}$$

$$\frac{\partial(\rho\varepsilon)}{\partial t} + \frac{\partial}{\partial x_j}(\rho U_j \varepsilon) = \frac{\partial}{\partial x_j} \left[\left(\mu + \frac{\mu_t}{\sigma_\varepsilon} \right) \frac{\partial \varepsilon}{\partial x_j} \right] + \frac{\varepsilon}{k} (C_{\varepsilon 1} P_k - C_{\varepsilon 2} \rho \varepsilon + C_{\varepsilon 1} P_{\varepsilon b})$$

In these equations C_μ , $C_{\varepsilon 1}$, $C_{\varepsilon 2}$, σ_k , and σ_ε are constants of the turbulence model. Now, P_{kb} and $P_{\varepsilon b}$ represent fluctuability forces and P_k is production of turbulence due viscous forces.

2.2. Particle Governing Equation

The forces that act in a particle traveling through fluid affect its acceleration due to differences between the velocities of the particle and fluid, as well as fluid dislocations over the particle. The movement equation for this particle, considering all forces acting in the system, was derived by researches Basset, Boussinesq, and Oseen and are shown in the equation:

$$m_p \frac{dv_p}{dt} = F_D + F_B + F_R + F_{VM} + F_P + F_{BA}$$

where F_D represents drag forces acting in particle, F_B is fluctuability forces due to gravity, F_R are rotational domain forces, represents mass force added, or virtual, F_P is gradient pressure forces, and F_{BA} is known as *Basset* term, that represents deviations in the standard flow.

The change rate of temperature is commanded by three physical processes: convective heat transfer, mass transfer and radiation. The change rate of temperature in the particle is obtained by a sum, shown in the equation:

$$\sum (m_C C_P) \frac{dT}{dt} = Q_C + Q_M + Q_R$$

where Q_C , Q_M , and Q_R are heat transfers for convection, mass, and radiation.

The instantaneous velocity calculations of fluid, v_p , depends on flow regime and kind of particles. For turbulence regime, the instantaneous velocity of fluid is decomposed in principal component, v_p , and fluctuant, v'_f . The turbulent dispersion of the particle is assumed in model that each particle is inside a single turbulent swirl, and that each swirl has fluctuant velocity, v'_p , duration, τ_e , and characteristic length, l_e , calculated by Gosman and Ioannides, as shown in the follow equations:

$$v'_f = \Gamma(2k/3)^{0.5}$$

$$\tau_e = \frac{l_e}{\left(\frac{2k}{3} \right)^{\frac{1}{2}}}$$

$$l_e = \frac{3}{\varepsilon} \frac{C_\mu^{\frac{3}{4}} k^{\frac{3}{2}}}{2}$$

where C_μ is the turbulence constant.

The aerodynamics drag force, F_D , over the particle is proportional to the flow velocity, U , between fluid and particle, as shown by the equation:

$$F_D = \frac{1}{2} C_D \rho_F A_F (U_F - U_P)$$

where C_D is the drag coefficient, A_F is the effective transversal particle section, and U_F and U_P are velocities of fluid and particle, respectively.

$$C_D = \max \left[\frac{24}{\text{Re}} (1 + 0.15 \text{Re}^{0.687}); 0.44 \right]$$

Now, buoyant force over the particle is the force acting in the particle immersed in the fluid, and can be described by the equation:

$$F_B = \frac{\pi}{6} d_p^3 (\rho_p - \rho_f) g$$

where d_p is the particle diameter, ρ_p is the particle density, ρ_f is the fluid density, and g is the gravity vector.

2.3. CO Combustion

During converter operation some amounts of environmental air enter by the skirt. The oxygen of this air reacting with carbon monoxide came from the furnace. This combustion model uses transport equation of mass fraction for the component Y_i :

$$\frac{\partial(\rho Y_i)}{\partial t} + \frac{\partial(\rho U_j Y_i)}{\partial x_j} = \frac{\partial}{\partial x_j} \left(\Gamma_{ie,f} \frac{\partial Y_i}{\partial x_j} \right) + S_i$$

where the source term S_i refers to the rate of chemical reaction involved, i component. Generally, the rate of production and consumption of S_i to i component can be computed as the sum of progress rates for all elementary reactions in which i participates, as the equation:

$$S_i = W_i \sum_{n=1}^N (v''_{ni} - v'_{ni}) R_n$$

where v_{ni} is the stoichiometric coefficient to the i component in the elementary reaction n , R_n is a rate of elementary reaction to the reaction n .

3. Material and Methods

3.1. Modeling Dedusting System

The computational analysis for the dedusting system was divided in four parts. The first simulation is based in the data gathered with the device actually in operation. In the second simulation the inner diameter was increased to 2,200 mm. Changes in joints were introduced in the third simulation, being the biggest change the curve located on the top of the system, where the joints were smoothed. In the fourth simulation, an extrapolation of dimensions to 2,900 mm was made (Fig. 1).

For a good approximation of the results with the information's collected in the operational area, an adaptation of the geometry by a no-structured mesh was used. This mesh is favorable to follow particles through Lagrangian descrip-

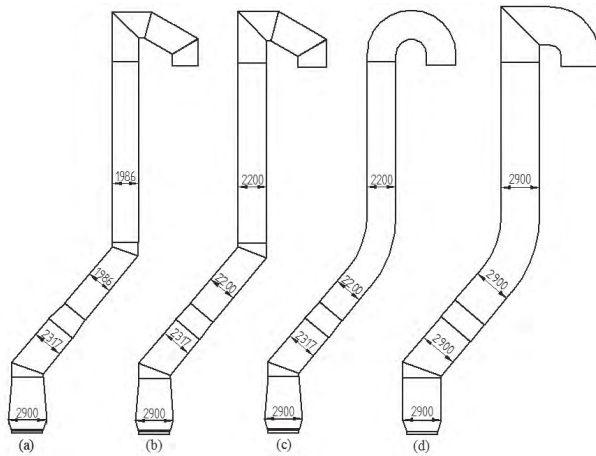


Fig. 1 Dedusting system dimensions, (a) actual; (b) change 1; (c) change 2, smoothing; and (d) change 4, extrapolation of the dimensions

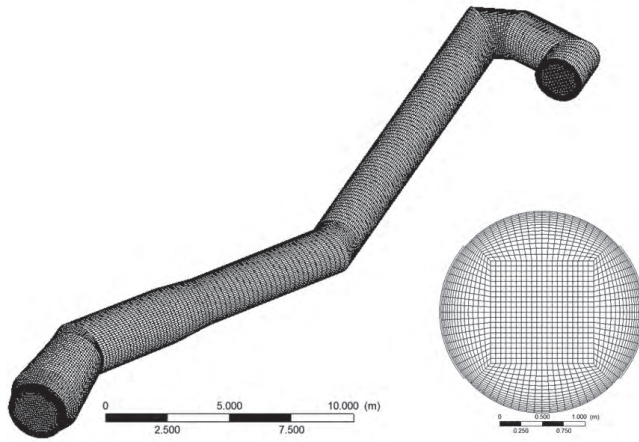


Fig. 2 Computational mesh with 400 thousand nodes and inlet detail

tion, individual following of particles considering gravity, drag's forces and turbulent dissipation.

A mesh with 400 thousand nodes, showed in Fig. 2, was used in the computational simulations.

The boundary conditions were adjusted with parameters collected from the operational area. In these simulations two different heights of the skirt were considered: completely closed to the converter's mouth and 100 mm above it. A second simulation was made for the cooling pipe system. By this simulation the equation that describe the behavior of the internal wall temperature, responsible for cooling fumes as a function of internal velocity, was obtained and is shown below:

$$T = \left(\frac{T_{\min} - T_{\max}}{L} \right) X + T_{\max}$$

where T_{\max} is the maximum temperature in the wall, T_{\min} is the minimum temperature, L is the total length of cooling stack, and X is the cartesian position. In the input of system a gas flow of 3,660 Nm³/min and a temperature of 1,700 °C were used. The pressure in the exit of the cooling pipes was established in 2,500 mmWC.

Table 1 Boundary conditions

	Units	Close skirt	Skirt 100 mm open
Gas Flow	[Nm ³ /min]	3,660	3,660
Particles Flow	[kg/s]	1.69	1.69
Ø Particles	[µm]	100	100
Gas Temperatures	[°C]	1,700	1,700
Enter pressure	[atm]	1	1
Enviromental temperature	[°C]	—	40
Exit pressure	[mmCA]	2,500	2,500
Water temperature	[°C]	80	80
Pipes roughness	[µm]	0.045	0.045

For the simulation with the skirt completely close, no air enters in the hood - only fumes flow through the dedusting system. When the skirt is open, air conditions are pressure at 1 atm and temperature 40 °C. Table 1 shows data used in the simulations. In the combustion factor of flammability used was equal to 0.42. This factor limits stoicmetric of equations and promotes adjusts in flame temperature.

4. Results and Discussion

The results will be shown considering first with the skirt completely closed and second with the skirt open 100 mm.

4.1. Flow with the Skirt Completely Closed

The results of profile temperature variations across the ducts and in the top of the dedusting system with the skirt completely closed presented the same behavior (Fig. 3).

For the same opening condition, the energy source programmed in the CFD was equal to the four cases. It is necessary to close the mass, energy, and chemical balances. In this way, the solver has the convergence and in this case, the top temperature is near the same in all cases. The temperature profile has small variations as function of the geometry, but there is compensation: when the duct diameter increases,

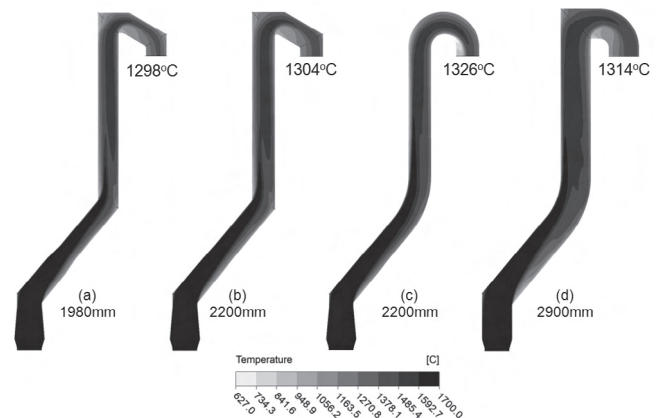


Fig. 3 Temperature profile with different diameters and shape of ducts

fume velocity decreases for the same exhaust capacity of the fan. By the fume convective heat transfer coefficient, when the fume velocity decreases, the convective power decreases too and the impact is under cooling capacity. For the system completely closed, the top end temperature has small variations.

In operational practice, the skirt completely closed does not occur. Little air infiltration takes place and oxygen reacts with carbon monoxide producing carbon dioxide; in the other side, nitrogen, an inert gas with high concentration in the air, promotes reduction in fumes temperature.

Still in Fig. 3, fluid flow causes alterations in temperatures yields proving that special care is necessary for cooling in the hood, skirt movable, and first 45° curve.

The inner diameter has strong influence in the flow velocity for the system completely closed. Fig. 4 shows different velocity profiles along the cooling system. It is possible to see in Fig. 4a that fast tapering in the inner diameter causes the fume velocity to increase. The high fume velocity has bad consequences in the 180° curve at top which accelerates pipe wear. When the inner diameter grows, as in Fig. 4b, average velocity comes down considerably and reduce turbulence in the 180° curve at the top.

The bigger difference between velocity profiles is due to the 180° curve at the top, when a smooth curve is developed velocity in the curve reduces significantly, as shown in Fig. 4c, when compared with cases (a) and (b). In (c) a new

concept promotes a best distribution of velocity across a section. This new condition contributes for next stage into dedusting system: wash the fumes. In Fig. 4d, the extrapolation case shows the ideal situation to obtain good life for the cooling pipes, low average velocity, and well distributed along the section that permits good conditions for the first stage to clean gases.

The Fig. 5 shows a section of duct at the height of 25 m.

It is possible to see that the fumes with high velocity have a strong contact with the pipes wall. When the diameter is increased and smooth geometry is applied, the velocity near the pipes wall reduces. This is good for the pipes lifetime, but it is not very good for heat transfer.

The fumes velocity has strong influence on the particles impact on the surface of the pipe walls. The gas flow drags the particles all the way through the system and as the gas velocity decreases, the velocity of the dragged particles also decreases. Fig. 6 shows the particles route monitored by Lagrangian discretization method. For the constant flow of particles, equal in all simulations, it is possible to observe the same impact regions, but the impact intensity is related to the particles velocity impact.

Fig. 7 shows the particles impact effect under surface of pipe walls in the 180° curve. When the curve is smooth, the impact region is less intensive than others. Increasing the inner diameter has the same influence.

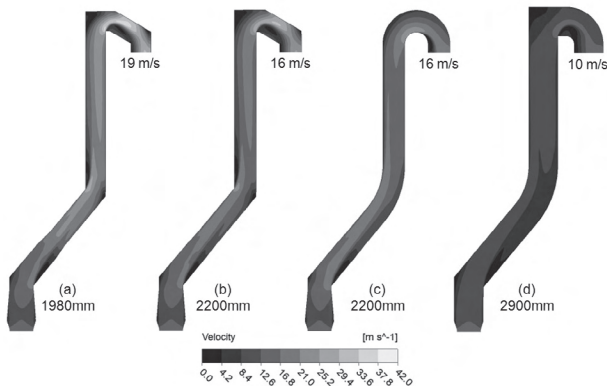


Fig. 4 Velocity profile

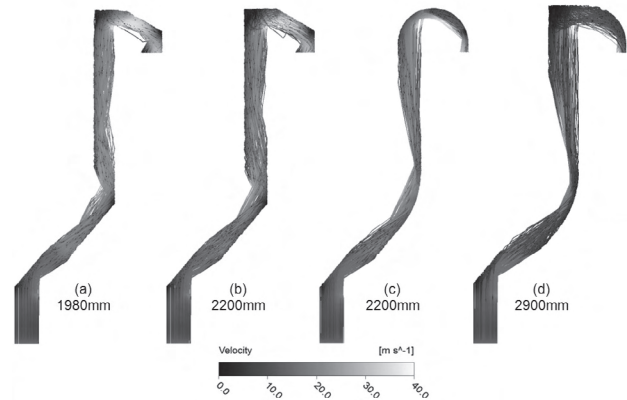


Fig. 6 Velocity along dedusting system

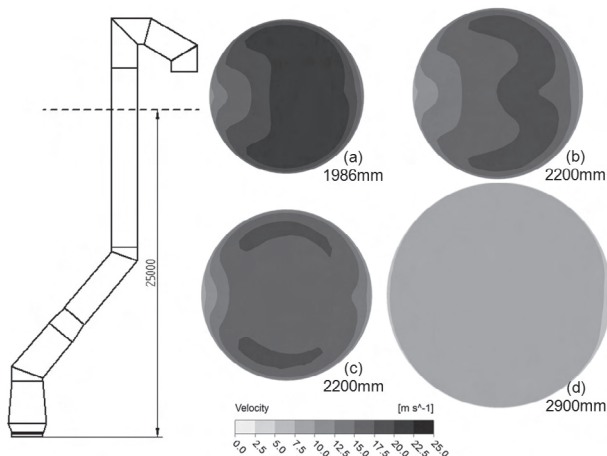


Fig. 5 Velocity profile in a section of 25 m above the mouth of the converter

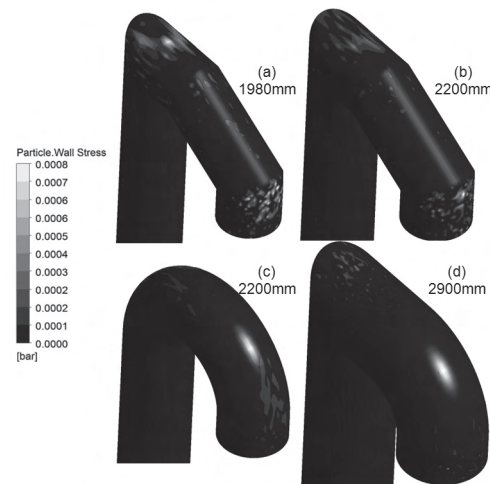


Fig. 7 Particle impact effect under the surface of the pipe walls

The profile (c) has the same diameter of profile (b), 2,200 mm. The difference in wall pressure is clear in the region where it is necessary to change the flow direction and reduce it with a smooth geometry. The profile (c) is the best design situation analyzed.

4.2. Flow with Open Skirt

When the skirt is open, air admission occurs into the hood. This air starts combustion along the cooling ducts and modifies gas chemical composition and temperature (Fig. 8).

The entrance air density is higher than the converter fumes forcing them to the center of the cooling stack. The air reacts with carbon monoxide, increases the carbon dioxide concentration and temperature along the ducts. The simulation results were verified with real industry values during maximum decarburization time indicating the compatibility between the CFD study and the real situation.

Comparing Fig. 9 and Fig. 6, it is possible to observe that the entrance air forced the fumes to the center of the duct resulting in a conical shape. With the change in duct slope and the gas flow centralization, the collision of particles is enhanced in specific regions of the hood and highlighted in Fig. 10.

The particles impact is also motivated by high temperature in the same regions. The results of this analysis coincide with the effects suffered in routine operations.

5. Conclusions

The main conclusions of this work are:

- For the closed system, the inner diameter increase reduces the fumes velocity, increasing the boundary layer near the pipe walls and reducing the heat transfers of the cooling system;
- For the open system, the temperature increases due to post combustion long the entire length of the ducts;

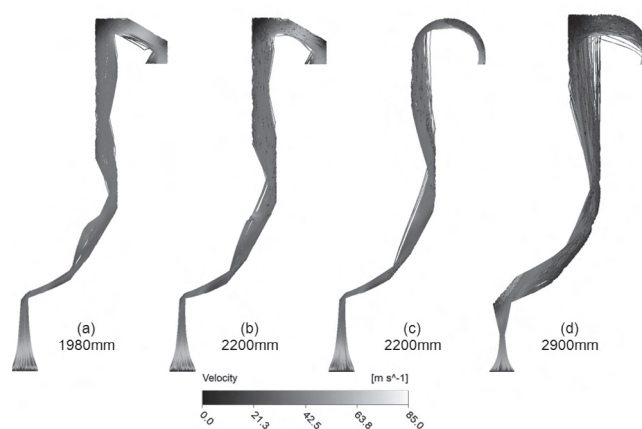


Fig. 9 Particles trajectory along cooling ducts

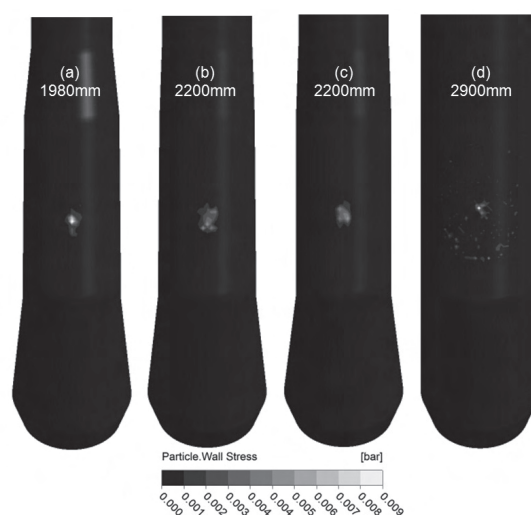


Fig. 10 Particles impact in the first curve of the dedusting system

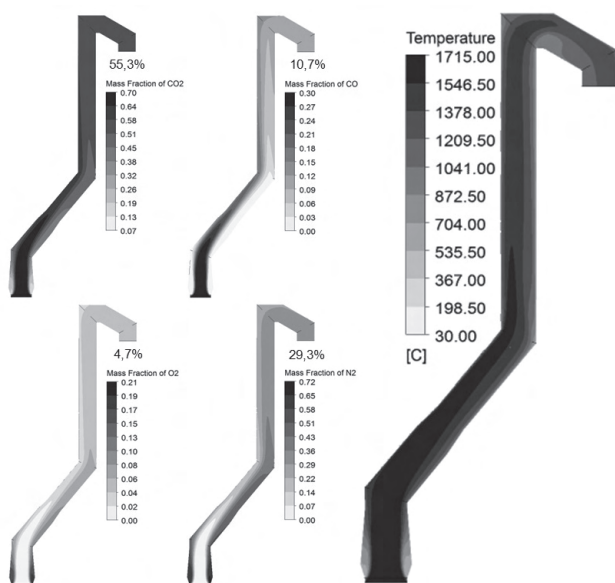


Fig. 8 Gas composition during combustion along the cooling ducts

- For open system, the entrance air with higher density compresses the hot gases and concentrate the impact areas on the stack;
- CFD shows gas analysis after post combustion very closed to the industry values.

REFERENCES

1. Schnelle KB, Brown CA. Air Pollution Control Technology Handbook. CCR Press, 2001.
2. Kerry FG. Industrial Gas Handbook: Gas Separation and Purification. CCR Press, 2006.
3. Shapiro HN, Moram MJ. Fundamentals of Engineering Thermodynamics. New York: John Wiley & Sons, 1988; p.417-35.
4. Perry RH, Green DW. Perry's Chemical Engineers Handbook. McGraw-Hill, 1997.
5. Innovative Turbulence Modeling: SST Model in ANSYS CFX. Technical Brief Ansys. Available from: <http://www.ansys.com>. [Accessed in 2006 Dec 29].
6. ANSYS Fluent. Fluent User's Guide, 2005.
7. Maliska CR. Transferência de Calor e Mecânica dos Fluidos Computacional - Fundamentos e Coordenadas Generalizadas. Rio de Janeiro: Livros Técnicos e Científicos, 1995.